Electron-Electron Scattering in Non-Parabolic Transport Models

Josef Gull, Lado Filipovic, and Hans Kosina
Institute for Microelectronics, TU Wien, Gußhausstraße 27–29, 1040 Wien, Austria
e-mail: josef.gull@tuwien.ac.at

2024 International Conference on Simulation of Semiconductor Processes and Devices (SISPAD) | 979-8-3315-1635-2/24/$31.00 ©2024 IEEE | DOI: 10.1109/SISPAD62626.2024.10733120

Abstract

Recently, a Monte Carlo algorithm for the solution of a two-particle kinetic equation has been developed. This equation treats both single-particle scattering mechanisms (electron-phonon scattering) and two-particle scattering mechanisms (electron-electron scattering) in a consistent manner [GK23]. In this work, we present the extension of the algorithm to non-parabolic bands and discuss a statistical enhancement algorithm.

Model

Investigating electronic transport in semiconductors with the Monte Carlo (MC) method is based on the calculation of multiple random propagation paths (trajectories) and the computation of sample mean values. Each trajectory comprises free flight segments determined by Newtonian mechanics and scattering events described by quantum mechanics.

The novelty in our approach is that for each time step, we calculate two trajectories simultaneously. Those two electrons are, apart from their single-particle scattering rate, affected by a two-particle scattering rate which determines when both particles will interact with each other. The final states occupied by the electrons after scattering is selected randomly from the distribution of the allowed transitions.

Non-parabolicity

For transport simulations in silicon at higher electric fields it is important to account for band non-parabolicity. For this, we use the Kane-dispersion relation

$$E(1+\alpha E) = \frac{\hbar^2 k^2}{2m}$$

where α is the non-parabolicity coefficient. As a consequence, the carrier transport mass becomes energy-dependent, which must be taken into account in the calculation of the free flight paths. In the evaluation of the final states after electron-electron scattering (EES), it is important to keep the total energy and momentum conserved in order to avoid nonphysical effects.

Electron-Electron Scattering Rate

The total EES rate is defined as the integral of the transition rate with respect to the final states, or after changing variables, with respect to the momentum transfer vector. In the case of a non-parabolic band, this integral can no longer be evaluated analytically and one has to resort to a rejection method. The goal is to construct an analytically integrable auxiliary function $w_{up} > w$, where w is the actual integrand representing the transition rate. In this way, an upper bound of the scattering rate $\Gamma_{up} > \Gamma_{\text{ee}}$ can be found. The acceptance probability $p_a = w/w_{up}$ along with a random number r_0 then decides whether an actual scattering event ($r_0 < p_a$) or a self-scattering event ($r_0 > p_a$) is selected.
Defining the final wave vectors as $\boldsymbol{k}_1' = \boldsymbol{k}_1 + \boldsymbol{q}$ and $\boldsymbol{k}_2' = \boldsymbol{k}_2 - \boldsymbol{q}$, the equation that simultaneously states momentum and energy conservation is of the form

$$E(\boldsymbol{k}_1 + \boldsymbol{q}) + E(\boldsymbol{k}_2 - \boldsymbol{q}) - E(\boldsymbol{k}_1) - E(\boldsymbol{k}_2) = 0\,.$$

Especially in the non-parabolic case, choosing the reference point as $\boldsymbol{k}_0 = (\boldsymbol{k}_2 + \boldsymbol{k}_1)/2$ considerably simplifies the problem. With $\boldsymbol{K} = \boldsymbol{k}_2 - \boldsymbol{k}_1$ and $\boldsymbol{p} = \boldsymbol{q} - \boldsymbol{K}/2$ the energy balance equation becomes

$$g(\boldsymbol{p}) := E(\boldsymbol{k}_0 + \boldsymbol{p}) + E(\boldsymbol{k}_0 - \boldsymbol{p}) - E(\boldsymbol{k}_1) - E(\boldsymbol{k}_2) = 0\,.$$

It turns out that the solution set of $g(\boldsymbol{p}) = 0$ is a rotationally symmetric ellipsoid. The short semi-axis is orthogonal to $\boldsymbol{k}_0$ and given by

$$b^2 = \frac{k_1^2 N_2}{4N_1} + \frac{k_2^2 N_1}{4N_2} - \frac{\boldsymbol{k}_1 \cdot \boldsymbol{k}_2}{2}\,,$$

where $N_{1,2} = 1 + \alpha E_{1,2}$. $N_3 = N_1 + N_2 - 1$ is another coefficient related to non-parabolicity. The long semi-axis is parallel to $\boldsymbol{k}_0$:

$$a^2 = \frac{b^2}{1-e^2}, \quad e^2 = \frac{2\alpha}{m}\left(\frac{\hbar k_0}{N_3}\right)^2$$

Note that the excentricity e vanishes in the parabolic limit.

Assuming Fermi's Golden rule and the matrix element for screened Coulomb interaction results in the following expression for the total scattering rate:

$$\Gamma_{\text{ee}} = A \int_{\mathbb{R}^3} \frac{\delta[g(\boldsymbol{p})]}{(|\boldsymbol{k}_1' - \boldsymbol{k}_1|^2 + \beta_s^2)^2} \mathrm{d}^3 p\,, \quad A = \frac{ne^4}{4\pi^2 \hbar \varepsilon_s^2}$$

Substituting $\boldsymbol{k}_1' - \boldsymbol{k}_1 = \boldsymbol{p} + \boldsymbol{s}$ with $\boldsymbol{s} = \boldsymbol{K}/2$ and assuming spherical polar coordinates with $\boldsymbol{K}$ as the polar axis, leads to

$$\Gamma_{\text{ee}} = A \int_0^{2\pi} \int_0^{\pi} \int_0^{\infty} \frac{\delta[g(\boldsymbol{p})] p^2 \sin\vartheta}{(p^2 + s^2 + 2\boldsymbol{p}\cdot\boldsymbol{s} + \beta_s^2)^2} \mathrm{d}p \mathrm{d}\vartheta \mathrm{d}\phi$$

Integrating with respect to p can be carried out with the help of the δ-function.

$$\Gamma = A \int_0^{2\pi} \int_{-1}^{1} w(\chi, \phi) \mathrm{d}\chi \mathrm{d}\phi \quad \text{with}$$
$$w = \frac{mp^3}{2\hbar^2 b^2} \frac{N_3 (1 - (e^2/k_0^2)(p^2 - b^2))}{p^2 + s^2 + \beta_s^2 + 2ps\chi}\,.$$

Since $p = p(\chi, \phi)$, which describes the ellipsoidal level-set, is a function of both angles, the integrand lacks azimuthal symmetry. We construct an analytically integrable upper bound $w_{up} > w$ using the inequality $b \le p \le a$

$$w_{up} = \Phi \frac{m}{\hbar^2} \frac{N_3 a^2}{b^2} \frac{2a}{(4b^2 + 4b^2\chi + 2\beta_s^2)^2}\,.$$

This function still contains an empirical parameter $\Phi > 1$ which has yet to be determined. By means of the following anti-derivative,

$$I(\chi) = 2\pi \int_{-1}^{\chi} \left(4b^2 + 4b^2\chi' + 2\beta_s^2)\right)^{-2} \mathrm{d}\chi'$$
$$= \frac{\pi(1+\chi)}{\beta_s^2 (4b^2(1+\chi) + 2\beta_s^2)},$$

the upper bound of the EES rate is readily obtained:

$$\Gamma_{up} = \Phi A \frac{\pi m}{\hbar^2 \beta_s^2} \frac{N_3 a^2}{b^2} \frac{2a}{4b^2 + \beta_s^2}$$

Computational experiments show that a value of $\Phi = 2$ is required to ensure $w_{up} > w$ on the whole unit sphere. An improved auxiliary function without such free parameter is currently being developed.

Final States after Electron-Electron Scattering

The cumulative probability distribution for ϑ is given by $p(\cos\vartheta) = I(\cos\vartheta)/I(1)$. Applying the inversion method yields an expression for the random polar angle ϑ. In spherical coordinates the direction of $\boldsymbol{p}$ with respect to $\boldsymbol{K}$ is defined by the two random numbers r_1 and r_2 as

$$\cos\vartheta = \frac{\beta_s^2 - r_1(4b^2 + 2\beta_s^2)}{\beta_s^2 + 4r_1 b^2}\,, \quad \phi = 2\pi r_2\,.$$

The magnitude of $\boldsymbol{p}$ is given by the equation for the aforementioned ellipsoid

$$p^2 = \frac{b^2}{1 - e^2 \cos^2\gamma},$$

where γ is the angle between $\boldsymbol{p}$ and $\boldsymbol{k}_0$. With probability w/w_{up} a physical EES event is chosen and the wave vectors are updated: $\boldsymbol{k}_1' = \boldsymbol{k}_0 + \boldsymbol{p}$, $\boldsymbol{k}_2' = \boldsymbol{k}_0 - \boldsymbol{p}$.

Statistical Enhancement

To study the high-energy tail of the energy distribution function (EDF), an algorithm that enhances the number of sampling points at higher energies is required. Although the cascaded splitting/gathering algorithm proposed by Phillips and Price [PJP77] is very successful in the case of the single-particle MC method [PJP77], for non-uniform electric fields it is not directly applicable to the two-particle MC method. Therefore, we devised a new method based on the notion that any stationary average can be viewed as a time average. An integral over the simulation time T is split into multiple integrals that we refer to as time frames. Within a time frame, the MC simulation, designated as traj. in Figure 1, can be repeated N-times, while the contribution to the averages is weighted by $1/N$. A time frame is repeated once an electron enters the rare domain (for instance, $E_{\text{tot}} > E_{\text{th}} \wedge x_l < x < x_r$, Figure 2). Then, N trajectories each with weight $1/N$ are simulated for the time frame duration t_f. Common trajectories are terminated at the end of each time frame, and rare ones are continued with adjusted weights.

Cascading

Applying the algorithm in cascade requires an appropriate data structure along with clearly defined methods for manipulation. We chose a tree with the following characteristics:

- Each node holds a Simulation State (i.e., the states of the sample electron and all partner electrons)

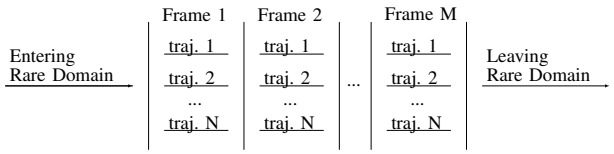

Fig. 1. Repeated time frame algorithm. A rare simulation state is calculated repeatedly for a certain period of time.

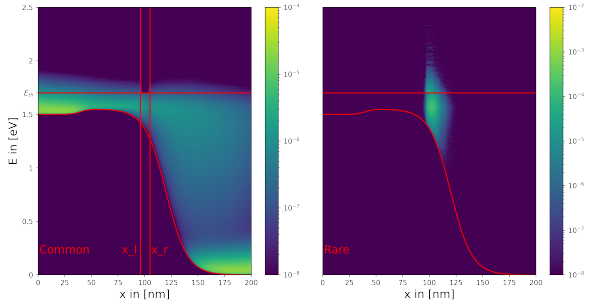

Fig. 2. Left: Distribution of common samples and boundaries of rare-zone. Right: Distribution of rare samples of the repeated time frame algorithm.

- A node has either N or 0 children.
- The weight of a node is given by $w_n = w_{\text{parent}}/N$.
- $w_{\text{root}} = 1\,, \quad \sum_{\text{leafs}} w = w_{\text{root}}$

The sequence of the algorithm is as follows:

1) Make a list of all leaf nodes
2) Simulate one time frame for each list entry, and determine if it is still of interest.
3) Restructure the tree, go to $\rightarrow 1$

For each level in the tree, there exists a corresponding energy threshold. Thus, a sample is of interest when the energy exceeds this threshold. In order to restructure the tree, we allow two methods: splitting and gathering. Whenever a leaf node is of interest, it is split, meaning that we add N child nodes to it and copy the Simulation State to all of them. Whenever all siblings of one leaf node are no longer of interest, they are gathered. Gathering means we copy the state from one of the siblings to the parent node and remove all siblings thereafter.

RESULTS

The conduction band structure of silicon is modeled by six equivalent isotropic valleys, characterized by a Kane-dispersion relation with $m = 0.3m_0$ and $\alpha = 0.5\text{eV}^{-1}$. Acoustic and intervalley phonon scattering is implemented according to [JL12]. To test our models, we simulate a potential barrier, similar to the surface potential of a MOSFET. If an electron leaves the device through a contact, a new one is injected with equal probability in the drain or source. The new electron state is obtained from an equilibrium box, which is a MC simulation on its own.

Figure 3 and Figure 4 show the energy distribution function in the parabolic and in the non-parabolic case, respectively. The color intensity correlates to the amount of samples. In domains with bright colors, the amounts of samples are the highest. The non-parabolic model leads to a faster decay of the electron energy in the drain region compared to the parabolic one. This effect is caused by an increase in the scattering rate at higher energies in the non-parabolic model.

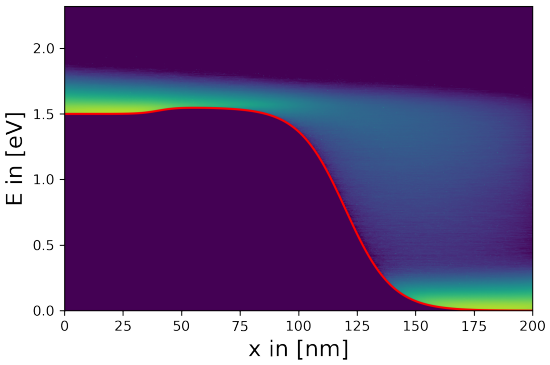

Fig. 3. Energy distribution function (EDF) for a parabolic dispersion.

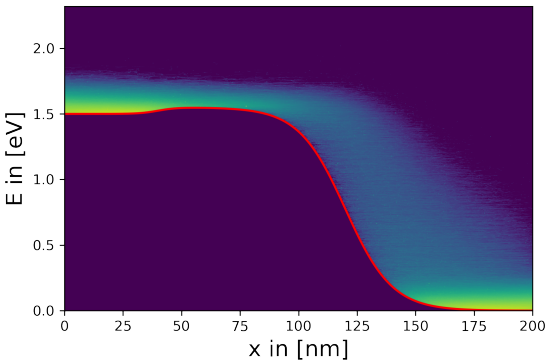

Fig. 4. EDF for a non-parabolic dispersion. A faster decay of the electron energy in the drain region is observed.

Figure 5 shows carrier density, mean energy, and mean velocity as well as the screening length $\lambda = \beta_s^{-1}$ across the device. We compared different initial carrier densities in the parabolic and non-parabolic models. As a reference, also a simulation without EES is included. Velocities and energies are smaller in non-parabolic

simulations due to higher scattering rates. The screening length in the channel appears to be $10-30$ times larger than in the contracts. In the parabolic case, we can also see that the mean energy is lower for higher initial carrier densities.

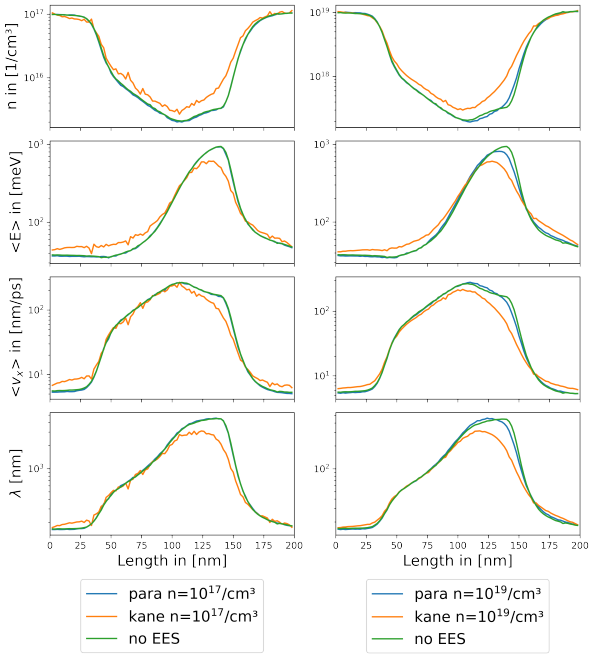

Fig. 5. Device characteristics for different simulation settings.

Figure 6 shows cut through the EDF in Figure 3 at $x = 100$nm. Since highly energetic electrons have the ability to harm the device, we are interested in the tails of the distributions. In the parabolic case, we can see that higher initial carrier concentrations enhance the tail. To increase the resolution in the high-energy tail the repeated time frame algorithm was used. Figure 7 shows the effectiveness of the algorithm. Here again a cut at 100nm is studied. Simulations were performed with (i) no enhancement, (ii) 100 repetitions above 1.7 eV and (iii), 1000 repetitions above 1.8 eV. It can clearly be seen that the algorithm produces more samples in the high-energy region and, therefore, reduces the statistical error in those domains.

Acknowledgment

The financial support by the Austrian Federal Ministry of Labour and Economy, the National Foundation for Research, Technology and Development and the Christian Doppler Research Association and the Austrian Science Fund (FWF) within project P35318 [10.55776/P35318] and doc.funds TU-DX [10.55776/DOC142] is gratefully acknowledged.

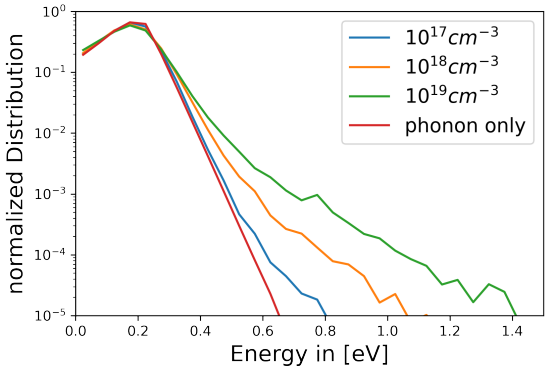

Fig. 6. EDF at position $x = 100$ nm. Enhancement of the high-energy tail scales with the carrier concentration as predicted by [CL96].

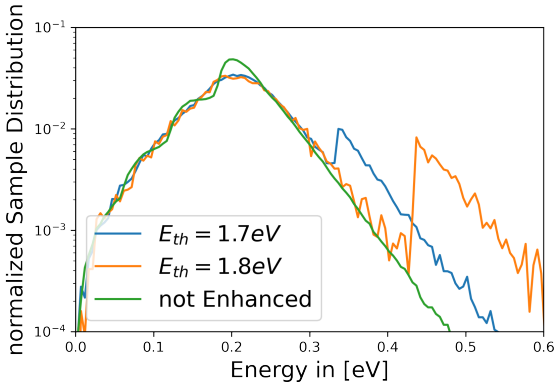

Fig. 7. Normalized sample distribution at $x = 100$ nm for $n = 10^{17}$ cm^{-3}, $E_{\text{th}} = 1.7$ eV with 100 repetitions and $E_{\text{th}} = 1.8$ eV with 1000 repetitions.

References

[CL96] P.A. Childs and C.C.C. Leung. "A one-dimensional solution of the Boltzmann transport equation including electron–electron interactions". In: *Journal of Applied Physics* 79.1 (1996), pp. 222–227.

[GK23] Josef Gull and Hans Kosina. "Monte Carlo study of electron–electron scattering effects in FET channels". In: *Solid-State Electronics* 208 (2023), p. 108730.

[JL12] Carlo Jacoboni and Paolo Lugli. *The Monte Carlo method for semiconductor device simulation*. Springer Science, 2012.

[PJP77] A Phillips Jr and PJ Price. "Monte Carlo calculations on hot electron energy tails". In: *Applied Physics Letters* 30.10 (1977), pp. 528–530.